Journal of the European Ceramic Society **13** (1994) 135–142

Porosity Development during Removal of Organic Vehicle from Ceramic Injection Mouldings

Heidi M. Shaw & Mohan J. Edirisinghe

Department of Materials Technology Brunel University, Uxbridge, Middlesex UB8 3PH, UK

(Received 8 July 1993, accepted 20 September 1993)

Abstract

Injection moulded test bars made using an alumina–polypropylene suspension were pyrolysed in air at 5 °C h⁻¹. Two types of test bars, with 50 and 57 vol.% alumina, were investigated. Mercury porosimetry has been used to monitor the development of surface and interconnected porosity in the test bars during the initial stages of pyrolysis when approximately 30 wt% of organic vehicle was removed. Pores detected have been grouped into three size ranges. Changes in the pore size distribution, which are shown to affect the four point bend strength of the pyrolysed test bars, have been explained in terms of various phenomena that take place during the removal of organic vehicle. Results reveal that the volume of porosity detected is much less than the expected total porosity. Shrinkage and redistribution of organic vehicle during pyrolysis are the major reasons for this. Therefore, during the initial stages of pyrolysis lack of sufficient surface and interconnected porosity could hinder the diffusion of degradation products of the organic vehicle and this is probably a major reason for the creation of defects in artefacts containing thick sections.

Spritzgußteststabe, hergestellt aus einer Aluminiumoxyd–Polypropylen-Suspension, wurden in Luft bei 5 °C h⁻¹ pyrolysiert. Zwei Typen von Teststaben mit 50 und 57 Vol% Aluminiumoxyd wurden untersucht. Die Entwicklung der Oberflächen- und Volumenporosität der Teststabe während des Anfangsstadiums der Pyrolyse, wenn etwa 30 Gew% des organischen Trägers entfernt waren, wurde mit Hilfe der Quecksilber-Porosimetrie bestimmt. Die gefundenen Poren wurden in drei Größenklassen unterteilt. Änderungen in der Porengrößenverteilung, die die Vierpunktbiegefestigkeit der pyrolysierten Stabe beeinflussen, konnten durch die verschiedenen Prozesse erklärt werden, die während des Entfernens des organischen Trägers stattfinden. Die Ergebnisse zeigen, daß das gemessene Porenvolumen wesentlich geringer ist, als die vermutete Gesamtporosität. Deshalb kann während des Anfangsstadiums der Pyrolyse ein Mangel an Oberflächen- und Volumenporosität die Diffusion der Reaktionsprodukte des organischen Trägers behindern, was wahrscheinlich der Hauptgrund für das Entstehen von Defekten in Produkten mit großem Querschnitt ist.

On a étudié la pyrolyse sous air à 5 °C h⁻¹ de barres moulées par injection à partir d'une suspension d'alumine et de propylène. On a examiné deux types de barres, l'une contenant 50 vol% d'alumine, l'autre 57 vol%. L'évolution de la surface et de la porosité ouverte dans ces barres a été suivie par porosimétrie au mercure, ceci durant les premiers stades de la pyrolyse, lorsque environ 30 pond% du milieu de suspension organique avait été éliminé. On a pu grouper les pores détectés en trois catégories de tailles. L'évolution de la distribution de taille des pores, dont on montre qu'elle joue sur la résistance en quatre points des barres pyrolysées, dépend de différents phénomènes qui se produisent lors de l'élimination du milieu organique de suspension. Les résultats montrent que la porosité détectée est très inférieure à la porosité totale prévue. Ceci est attribué essentiellement au rétrécissement et à la redistribution du milieu organique lors de la pyrolyse. Ainsi, une surface et une porosité ouverte trop faibles semblent empêcher la diffusion des produits de la dégradation du milieu organique durant les premiers stades de la pyrolyse; ceci explique vraisemblablement la formation de défauts dans certains échantillons épais.

1 Introduction

Many novel plastic forming methods, such as injection moulding,[1] vacuum forming[2] and blow moulding[3] are currently being developed for the fabrication of engineering ceramic artefacts. However, all these suffer from the fact that the organic vehicle used to enable shaping of the ceramic powder has to be subsequently removed, mainly by slow

Journal of the European Ceramic Society 0955-2219/94/$7.00

pyrolysis, before sintering the ceramic. Removal of organic vehicle frequently disrupts the arrangement of ceramic powder particles, especially in thick (~10 mm) sections,[4,5] and the resulting defects are a major problem in plastic forming operations.[6,7]

Practical organic vehicles contain several components[1] and their removal during pyrolysis involves degradation and evaporation.[8,9] Chain scission occurs in high molecular weight polymers such as polypropylene and the resulting degradation products diffuse to the surface of the moulding and evaporate. The presence of oxygen causes oxidative degradation in the surface regions, in addition to thermal degradation in the core of the mouldings. Therefore, under these conditions, preferential loss of organic vehicle could occur in the surface regions.[10] In addition to these reactions, low molecular weight constituents, such as waxes, added as flow modifiers and processing aids, diffuse to the surface and evaporate.

Two theoretical mechanisms by which the removal of the organic vehicle takes place, creating porosity, have been identified.[11,12] The first occurs when the organic vehicle front recedes into the ceramic body whilst remaining a continuous phase. Therefore, porosity forms from the surface inwards as a continuous outer layer. The second mechanism involves the formation of porosity throughout the body as low molecular weight constituents and degradation products of the organic vehicle diffuse to the surface. This causes redistribution of the organic vehicle. In practice, a combination of both mechanisms can be expected to occur. However, in an oxidising atmosphere, where preferential removal of the organic vehicle could occur in the surface regions of the moulding, the first mechanism could be expected to dominate during the early stages of pyrolysis. A combination of mechanisms one and two could also result in the presence of interconnected pores between the surface and interior regions of the ceramic body.

Gaseous diffusion of degradation products across a pore is several orders of magnitude faster compared to diffusion in the bulk polymer.[13] In fact, Matar *et al*.[12] have shown theoretically, with a single organic vehicle which degrades to monomer only, that if the first and second mechanisms operate separately, the critical heating rate of pyrolysis is increased by a factor of 2 and 2·7, respectively, compared with the situation where no porosity prevails. The presence of interconnected porosity throughout the moulding will further enhance diffusion and allow the use of faster heating rates during pyrolysis without creating defects such as bubbles in the ceramic body due to the excessive vapour pressure of degradation products.[14]

Porosity development is most helpful for mass transfer during the initial stages of heating when the viscosity of the organic vehicle is high and the diffusion coefficients of organic vehicle degradation products are low. In a previous communication[15] it has been shown, using potassium permanganate infiltration of pyrolysed test bars, that surface and interconnected porosity forms during the early stages of removal of the organic vehicle. However, a quantitative assessment of this porosity was not reported. The purpose of the present investigation is to quantitatively assess porosity development during the initial stages of pyrolysis when approximately 30 wt% of the organic vehicle is removed.

2 Experimental Details

2.1 Preparation of ceramic suspensions

Two formulations A and B containing 50 and 57 vol % of A16.SG alumina (Alcoa Manufacturing (GB) Ltd, Worcester, UK), respectively, were prepared using an isotactic polypropylene based organic vehicle. Microcrystalline wax and stearic acid were the other constituents of the organic vehicle. The particle size distribution and a scanning

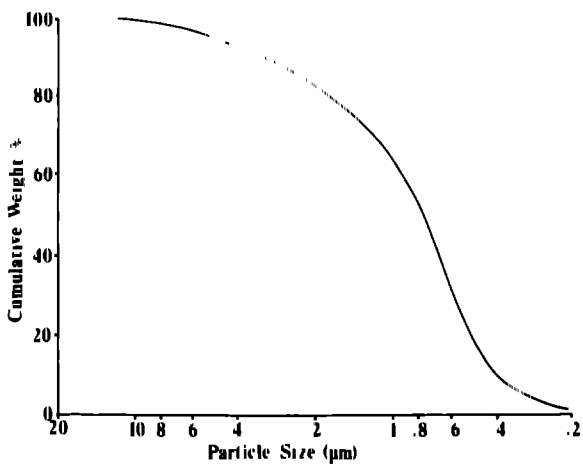

(a)

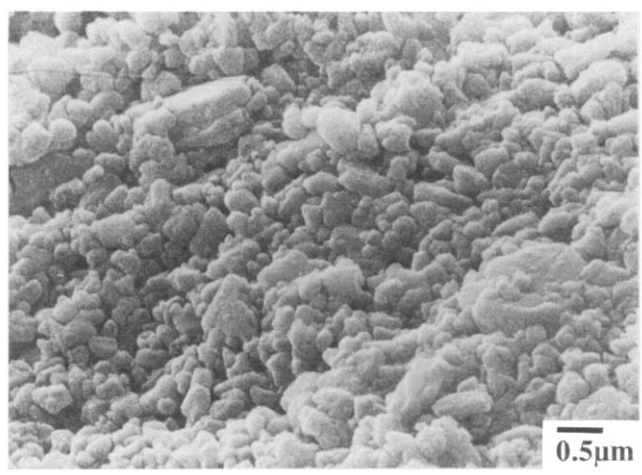

(b)

Fig. 1. (a) Particle size distribution and (b) shape of the ceramic powder used

Table 1. Details of each constituent in the binder system

Constituent	*Source*	*Density (kgm^{-3})*
Isotactic polypropylene grade GYS4SM	ICI Ltd Welwyn Garden City, UK	905
Microcrystalline wax grade 1865Q	Astor Chemicals Ltd, West Drayton UK	910
Stearic acid	BDH Chemicals Ltd Dagenham UK	941

Table 2. Compounding conditions

Screw diameter (mm)	40
Screw length diameter ratio	17
Screw speed (rpm)	60
Barrel temperatures (°C) Feed to exit	220–225–235–225

electron micrograph of the batch of ceramic powder used are given in Fig. 1(a) and (b). Details of each constituent of the organic vehicle are given in Table 1. The polypropylene, microcrystalline wax and stearic acid were mixed in the weight ratio 6:2:1. Preblends of each formulation (2 kg) were prepared by tumbling in a container for 5 min. The preblends were compounded in a twin screw extruder (Model TS40, Betol Machinery, Luton, UK) according to the conditions given in Table 2. The extrudates were dried and granulated and four samples of each formulation were heated to 600°C (ashing) to verify the volume of ceramic powder present.

2.2 Injection moulding

Granules of each formulation were used as feed stock for injection moulding. Tensile test bars 3 mm thick (Fig. 2) were produced from both formulations using a 6GV/50 Sandretto reciprocating screw injection moulding machine according to the conditions given in Table 3. The test bars were X ray radiographed before pyrolysis to check for the presence of voids and cracks.

2.3 Pyrolysis

Test bars were heated in a muffle furnace in static air according to a pre-determined temperature ramp that does not produce voids or cracks in the mouldings. The initial heating rate was 50°C h^{-1} up to 148°C (a few degrees below the dilatometric softening point of the formulations) followed by soaking for 24 h at this temperature. Subsequently,

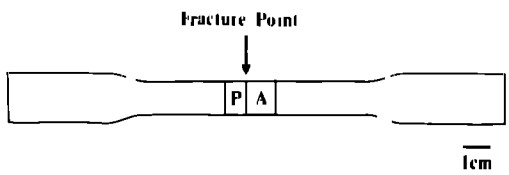

Fig. 2. Dimensions of as moulded test bar, indicating samples used for loss on ignition experiments and porosimetry.

Table 3. Injection moulding conditions

Injection pressure (MPa)	127
Barrel temperatures (°C) Feed to nozzle	195–210–225–235
Mould temperature (°C)	50

heating was continued at 5°C h^{-1}. Test bars were heated to 155, 170, 180, 195, 210, 225 and 240°C before cooling in the furnace to room temperature. Three test bars were pyrolysed to each temperature and were used to carry out the experiments described in Section 2.4 in triplicate. Test bars were X ray radiographed after pyrolysis to confirm the absence of voids and cracks. Each test bar was weighed before and after pyrolysis.

2.4 Testing

2.4.1 Strength

Test bars pyrolysed to each final temperature (see Section 2.3) were subjected to four point bend testing using an Instron machine with a load cell of 1 kN. Testing was carried out at room temperature (23 ± 2°C). A crosshead speed of 10 mm min^{-1} and a load span of 63 mm were used. Samples A and P from each fractured test bar (Fig. 2) were used in ashing and porosimetry experiments described in the following sections.

2.4.2 Loss on ignition

Sample A of each test bar was heated to 600°C to determine the weight of organic vehicle removed at each temperature investigated. This would verify the loss of organic vehicle detected from the weighing of test bars.

2.4.3 Porosimetry

Porosity was measured in two stages. In both instances sample P was the maximum size that could be tested in the porosimeters used. Firstly, the volume fraction and size distribution of pores with a radius < 7500 nm were measured using a Macropore Unit 120 (Carlo Erba, Milan, Italy). The sample was placed in a vial which was connected to a capillary. The vial was evacuated for about 10 min and mercury was dripped slowly into it through the capillary up to an indicated level. Subsequently, air was gradually allowed into the vial and mercury, now under pressure, was forced into the pores in the sample. Eventually, atmospheric pressure was reached and the change in height of the mercury in the capillary was recorded.

Higher pressures are needed to measure the volume fraction and size distribution of pores with a radius < 7500 nm and for this purpose the vial containing the sample and mercury was transferred to the autoclave of a computer controlled Porosimeter 2000 (Carlo Erba, Milan, Italy). The computerised system applied pressure to the mercury up

to 200 MPa (upper limit of this unit), intruding it into the pores of the sample Subsequently, pressure was released, causing mercury to extrude and thereby measuring hysteresis effects The intruded volume of mercury was used by the computer to calculate the volume fraction of pores and the pore-size distribution using a cylindrical model.

Both stages of porosity measurement were also repeated without a sample to correct for the mercury being subjected to compression during the testing.

3 Results and Discussion

3.1 Formulations

Ashing results showed that formulations A and B contained 81·24(±0·05) and 85·17(±0·14) wt% of ceramic powder, respectively. Assuming that the constituents of the organic vehicle were in the same proportion as blended, this is equivalent to 49 7 and 56·7 vol % of ceramic in formulations A and B, respectively

3.2 Weight loss

Figure 3 shows the weight loss of organic vehicle in formulations A and B as pyrolysis proceeds. Weighing of test bars and loss on ignition results produce almost identical weight loss curves In formulation A, which contains a higher initial amount of organic vehicle, there is a marked increase in weight loss at approximately 210°C. In comparison, formulation B loses weight more gradually over the pyrolysis temperature range investigated Two reasons can be attributed to this behaviour.

Firstly, in the oxidative pyrolysis atmosphere used, the surface regions of the test bars could be expected to lose a larger amount of organic vehicle, in comparison with the core region, as discussed earlier However, it has recently been shown[16] by molecular weight determinations and loss on ignition results of surface and core samples of

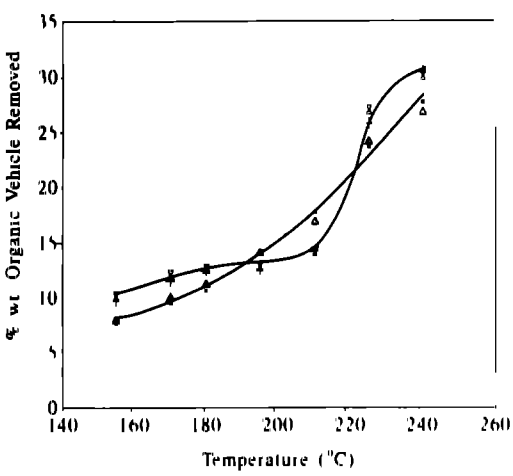

Fig. 3. Weight loss from test bars of formulations A (+, weighing; ⧖, ashing) and B (■, weighing, △, ashing) during pyrolysis

pyrolysed test bars that there is appreciable redistribution of organic vehicle during the initial stages of heating In particular, migration of microcrystalline wax from the core to the surface regions occurs during the early stages of pyrolysis and this is more predominant in formulation A.[16] Capillary migration of low molecular weight constituents of the organic vehicle in tape castings and injection mouldings has also been confirmed by optical microscopy.[13,15,17] Secondly, since formulation B contains a higher volume fraction of ceramic, this can catalyse the degradation of the organic vehicle[18] giving rise to a higher rate of weight loss at lower temperatures.

3.3 Porosity development

Several methods are available for the characterisation of porosity in powder compacts and these have been reviewed recently by German.[19] Mercury porosimetry is one of these methods and has been used frequently in assessing the pore sizes and pore-size distributions in both as formed and partially sintered ceramic bodies (e.g. Refs 20–23) It is a very useful technique for obtaining a comparative quantitative analysis,[19] as in this investigation, but a cylindrical pore shape is assumed throughout.

Porosity determination using the Macropore Unit showed that pores having a radius ·7500 nm were not present in any of the pyrolysed test bars.

Investigations using the Porosimeter 2000 resul ted in penetration volume versus applied pressure graphs (as shown in Fig. 4) Up to point A pores having radii of down to 100 nm are filled. As more pressure is applied, a further small increase in penetration volume results (region AB in Fig. 4) when pores down to 1000 nm are filled with mercury. The smallest pores (radii down to 3 nm) are filled when the pressure is increased further from about 10 to 200 MPa (region BC) The intrusion–extrusion cycle does not close on release of pressure and some mercury is always entrapped in the sample.

It is possible that pores with a radius · 3 nm are present but similar previous work on removal of organic vehicle from tape castings has shown that the characteristic pore size is in the range 70–90 nm.[11] It is also useful to compare the limit of 3 nm with the smallest hole in the pore architecture of the particle assembly in the ceramic body. For close-packed uniform size ceramic spheres of radius r this value (p) is $0{\cdot}155r$.[24] In the present situation, the exact pore size cannot be determined, mainly because the ceramic powder used is neither monodisperse nor spherical (Fig. 1(a) and (b)). Also, the condition of ideal close packing does not apply to commercial powders, such as the A16 alumina used in this investigation, in most fabrication processes. However, even in the ideal situation described,

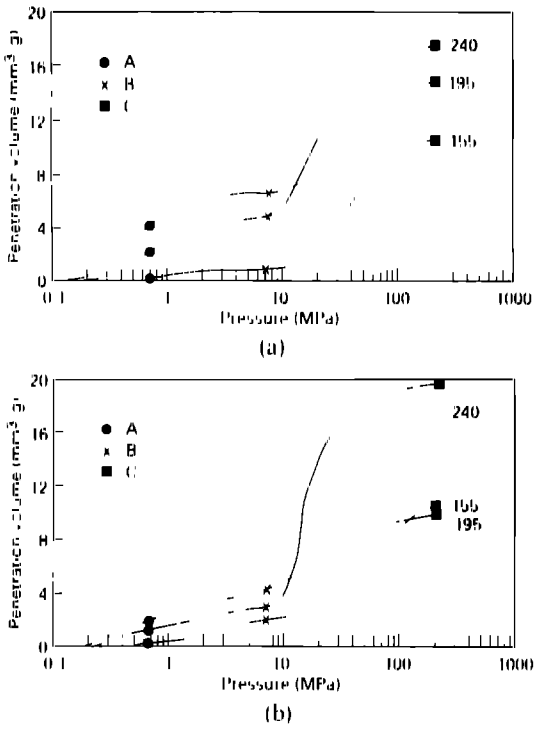

Fig. 4. Examples of penetration volume vs applied pressure curves of pyrolysed test bars of (a) Formulation A, (b) Formulation B. The temperature to which test bars were heated are indicated in the figures.

considering the variation of particle size from 10 to 0.2 μm (Fig. 1(a)), the range for p is from 775 to 16 nm, much larger than 3 nm.

Macro-defect free as-moulded test bars are not expected to show any porosity and this is consistent with the processing, as injection of molten suspension into a cavity under high pressure is expected to be pore-free[25] and, indeed, previous work[15] on the infiltration of potassium permanganate into mouldings confirmed this. Also, heating to the softening point of the suspension is largely to relieve residual stresses caused by injection moulding[26] and is carried out under fast heating rates,[27] usually with a negligible weight loss. In the present investigation, heating to a few degrees below the softening point of 148°C resulted in weight losses of only 0.6 and 0.52 wt% in formulations A and B, respectively, and this is negligible compared to the loss of organic vehicle at the temperatures investigated (Fig. 3). Therefore, heating to the softening point of the test bars is not expected to show any detectable porosity and in this investigation only mouldings heated to above the softening point were used for porosimetry.

It has been stated that the volume fraction of porosity, V_v, at any stage during pyrolysis is given by[12]

$$V_v = (1 - V_c)(1 - h)$$

V_c is the initial volume fraction of ceramic and h is the weight fraction of the remainder organic vehicle. Thus, the expected total porosity as organic vehicle is removed in formulations A and B are shown in Fig. 5(a) and (b), respectively. The experimentally

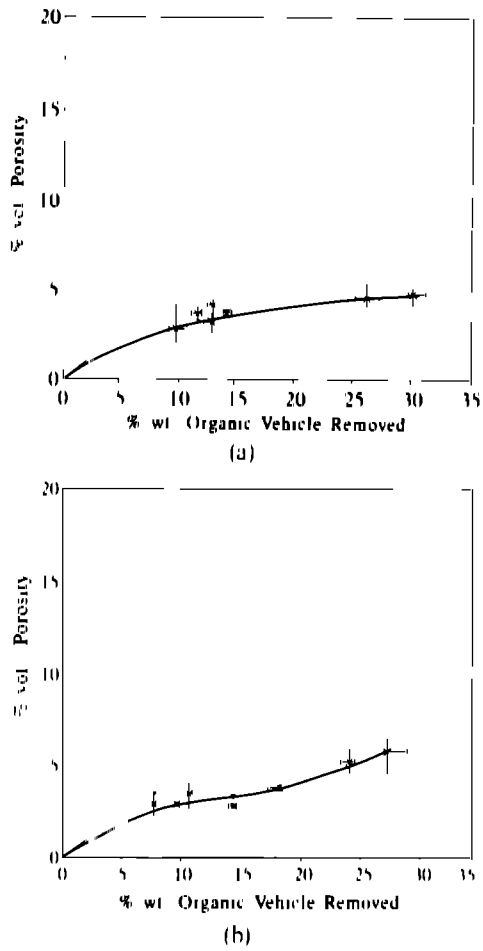

Fig. 5. Volume of porosity detected as a function of organic vehicle removed in (a) formulation A, (b) formulation B. — Expected total porosity, ×, measured porosity.

observed porosity from mercury porosimetry results are also shown in these figures. These results clearly show that the experimentally observed porosities are much less than the values expected during the initial stages of pyrolysis investigated. Clearly, the experimental observations include only surface and interconnected porosity. However, as discussed earlier, it is this type of porosity that is most effective in accelerating the diffusion of the degradation products of the organic vehicle.

There are two major reasons for this type of porosity to be almost 1/3 of the expected total porosity. Firstly, shrinkage occurs during pyrolysis and ceramic particles in the suspension move towards each other, increasing V_c.[28] This means that removal of organic vehicle does not directly result in an equal volume of porosity. Secondly, the migration of microcrystalline wax from the core of the mouldings to the surface regions, as discussed earlier, would result in the reduction of interconnected porosity. At a lower initial volume fraction of ceramic (formulation A) the shrinkage is greater,[28] and the redistribution of organic vehicle occurs over a wider temperature range,[16] and therefore the difference in expected and observed porosities will be larger, compared with formulation B, as shown in Figs 5(a) and (b). In formulation B,

after about 18 wt% of organic vehicle is removed, porosity does increase, to lower the difference between expected and observed values (Fig. 5(b)). Previous work[29] has shown that shrinkage due to removal of organic vehicle can decrease and reach a limiting value during the early stages of pyrolysis and this would happen earlier in formulation B in which the higher volume fraction of ceramic results in more efficient particle packing. This, and the fact that migration of microcrystalline wax was less pronounced in formulation B,[16] explains the more rapid increase in porosity after about 18 wt% of organic vehicle is removed. A similar increase in observed porosity in formulation A could be expected later on during pyrolysis when shrinkage is expected to decrease, but as this suspension contains a lower ceramic content (50 vol%), at the rate of heating used, this event probably occurs after the maximum loss of organic vehicle investigated (approximately 30 wt%) in the present work.

The pore size distributions present in the samples tested were analysed by classifying the pores formed into three size ranges:

7500–1000 nm: Large pores
1000–100 nm: Intermediate pores
100–3 nm: Small pores

These size ranges were identified because they seem to demarcate the three regions of mercury intrusion (Fig. 4) discussed in Section 3.3. Previous classifications in other types of investigations are not suitable for the present work. For example, the classification of pores according to their equivalent radii was proposed by Dubinin.[30] However, macropores were considered to have an equivalent radius > 100–200 nm and therefore this classification is unsuitable for this work. Zheng & Reed[22] working on sintering of powder compacts classified porosity present as a function of average particle diameter (d) of the ceramic powder used. The size of fine micropores and macropores were considered to be > $d/2$ and > $10d$, respectively. Taking d as 0·8 μm for the powder used in this investigation (Fig. 1(a)) the size of fine micropores and macropores would be > 400 nm and > 8000 nm, respectively. Therefore, once again this classification is unsuitable for the present work.

As shown in Fig. 6, in formulation A, at 155°C, > 90% of the porosity is in the < 100 nm size range. Therefore, the onset of oxidative degradation at the surface and the resulting weight loss from a negligible amount at the softening point to ~ 10% at 155°C results in the creation of small pores. A higher fraction of large and intermediate size pores are created as weight loss increases. This has also resulted in a decrease in the bend strength of the test bars. Between 170 and 180°C there is only a small increase in the percentage of large pores and this is because there is no significant change in the weight of organic vehicle removed in this formulation (Fig. 3).

At 195°C there is a bigger increase in the percentage of large pores present at the expense of a compensating decrease in intermediate pores. The authors' previous work[16] has shown that migration of microcrystalline wax in the organic vehicle to the surface regions of the mouldings is most significant at this temperature for this formulation. The well known Young & Laplace equation[31] indicates that the suction pressure of a pore is inversely proportional to its radius. Thus 'fluid' (in this case microcrystalline wax) could be sucked from the large pores into the intermediate size pores. According to the work of Shaw,[32] which describes the distribution of liquids in porous bodies, minimisation of free energy requires fluid to eventually fill the smallest pores in the body without distributing homogeneously. However, Shaw's work[32] is valid for the distribution of liquids in porous bodies under equilibrium conditions and, therefore, under a dynamic situation such as in the present investigation, this may not be possible, as capillary flow has to overcome the viscous forces in the molten suspension and the increase in ceramic particle packing due to shrinkage. During the early stages of pyrolysis, lower temperatures result in a high melt viscosity which is known[33] to retard capillary migration.

Overall, between 180 and 210°C there is no significant change in the pore size distribution and therefore the bend strength remains virtually unchanged. Figure 6(a) also indicates a substantial decrease in the percentage of large pores in the temperature range 210–240°C. In this temperature range the percentage of small pores increases. Figure 3 shows that at approximately 210°C loss of organic vehicle shows a rapid increase. Molecular weight determinations carried out on the suspension indicate[16] that at about 225°C extensive degradation of the polypropylene, which is the major constituent in the organic vehicle, occurs in the surface regions of the mouldings. This could be expected to produce a flurry of small pores and the degradation products, which are transported by diffusion in the liquid phase,[14] could also fill the large pores. This substantial decrease in the percentage of large pores causes the bend strength to increase slightly (Fig. 6(a)).

The changes in pore size distribution in the pyrolysed test bars of formulation B (Fig. 6(b)) show a similar trend to that of formulation A (Fig. 6(a)). However, a few differences are noticeable and these are now discussed. At 155°C, a higher fraction of intermediate size pores are present, although > 80%

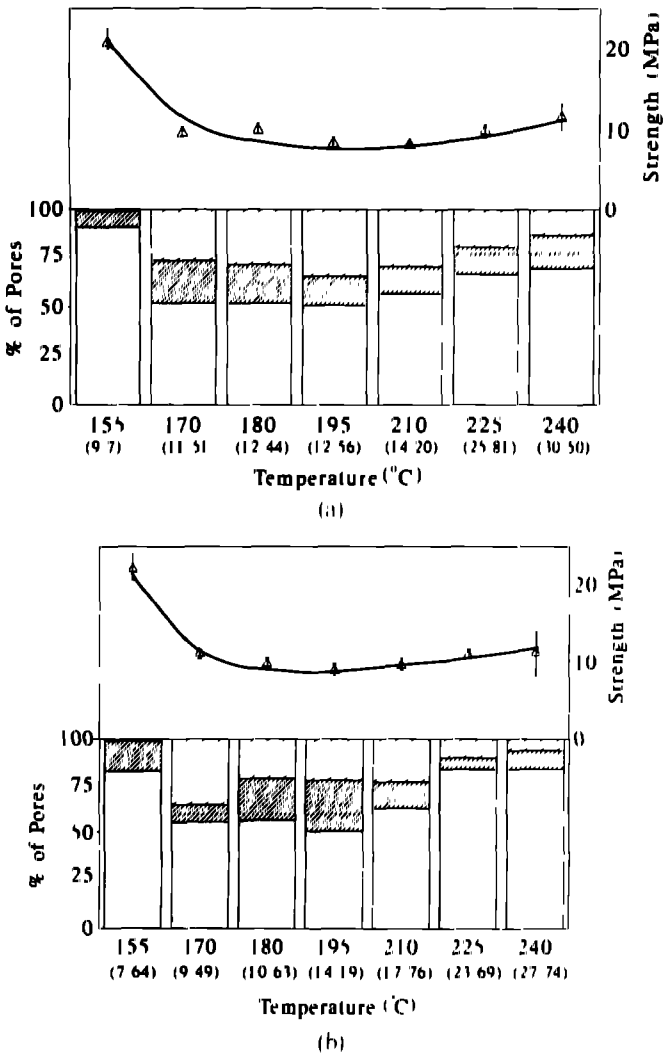

Fig. 6. Pore size distribution (□ large, ▨ intermediate, ■ small) and bend strength (△) of pyrolysed test bars of (a) formulation A, (b) formulation B. The average loss (in wt%) is given in parentheses below each temperature.

are fine pores. This is despite the fact that at 155 °C this formulation shows a lower weight loss. However, formulation B has a higher volume fraction of ceramic and the expected shrinkage due to removal of organic vehicle is therefore smaller compared to that of formulation A.[28] Therefore, any reduction of porosity due to shrinkage is less significant in formulation B and as a consequence larger pores can be expected.

Compared with formulation A, a higher percentage of large pores are present in formulation B at 170 °C. Migration of microcrystalline wax from the core to the surface regions occurs at a lower temperature (~170 °C) in this formulation[16] and, therefore, for reasons similar to those described for formulation A, this helps the formation of large pores in addition to those created due to the increase in weight loss. However, subsequent loss of organic vehicle, the rate of which is greater in formulation B compared with formulation A, causes an increase in the percentage of firstly intermediate size and subsequently fine pores. In fact, this could well be due to the evaporation of the microcrystalline wax which migrated from large pores to intermediate size pores by capillary action at 170 °C. In the temperature range 210–240 °C, the onset of extensive degradation of polypropylene present in the surface regions of the mouldings causes an increase in the percentage of small pores present, as in formulation A.

The major changes in pore size distribution during pyrolysis of these two formulations are similar and causes an almost identical variation in bend strength (Fig. 6(a) and (b)). This type of ceramic–polymer formulation has a typical flexure strength in the region of 12–15 MPa[34] and compact strengths of up to 14 MPa are possible during removal of organic vehicle.[35] The initial drop in bend strength from about 20 MPa to about 10 MPa takes place between 155 and 170 °C due to a marked increase in large pores. Thereafter, an appreciable percentage of large pores (20–30%) are present in both formulations up to about 210 °C and the bend strength is virtually unchanged (about ~10 MPa). The subsequent slight increase in bend strength measured at 225 °C and 240 °C is probably due to the substantial decrease in the fraction of large pores in both formulations as flurries of small pores appear due to the onset of extensive degradation of the polypropylene in the surface regions of the mouldings, as explained earlier.

4 Conclusions

The volume of surface and interconnected porosity developed during the initial stages of pyrolysis of injection moulded test bars is significantly less than the total volume of porosity expected. In the present investigation, where a polypropylene–microcrystalline wax–stearic acid organic vehicle was used in a formulation containing 50 vol% of alumina, porosimetry has shown that the first 30% of weight loss resulted in only 5 vol% of surface and interconnected porosity, which is only about 1/3 of the total porosity expected from theoretical calculations. Shrinkage, which causes further packing of ceramic particles, and redistribution of the organic vehicle, in particular migration of the low melting point microcrystalline wax to the surface regions of the mouldings, during the initial stages of pyrolysis are two major reasons for this effect. The lack of interconnected porosity during the initial stages of heating when diffusion coefficients are low would hinder the movement of degradation products of the organic vehicle and explains why this stage in the manufacture of thick section ceramic components using plastic forming operations frequently suffers from the creation of strength limiting defects.

It is also shown that the volume of porosity

detected and changes in the pore size distribution during the initial stages of pyrolysis were not significantly dependent on the initial volume fraction of ceramic in the suspension. In general, the onset of oxidative degradation when heated above the softening point of the suspensions causes the formation of small pores. Larger pores appear with subsequent weight loss and this is also helped by the capillary migration of microcrystalline wax. The degradation of the major constituent in the organic vehicle, polypropylene, in the surface regions of the test bars in the temperature range 210–240°C creates a flurry of small pores and results in a marked decrease in the percentage of large pores. The major changes of the pore size distribution are accompanied by variations in the bend strength of the test bars

Acknowledgements

The authors are extremely grateful to SERC for financial support of this research They also wish to thank Mr K K Dutta, Mr G. Raghir, Mr H Andrews and Mr S. Greenberg (Chemistry Department) for technical assistance. Mrs K. Goddard is thanked for typing the manuscript

References

1 Edirisinghe, M J, Fabrication of engineering ceramics by injection moulding, *Bull Amer Ceram Soc*, **70** (1991) 824–8
2 Haunton, K M, Wright, J K & Evans, J R G, The vacuum forming of ceramics *Brit Ceram. Trans J*, **89** (1990) 53–6
3 Hammond, P. D & Evans, J R G, On the blow moulding of ceramics *J Mater Sci Lett*, **10** (1991) 294–6
4 Bandyopadhyay, G & French, K W, Injection molded ceramics' critical aspects of the binder removal process and component fabrication *J Eur Ceram Soc*, **11** (1993) 23–34.
5. Evans, J R G & Edirisinghe, M J, Interfacial factors affecting the incidence of defects in ceramic mouldings *J Mater Sci*, **26** (1991) 2081–8.
6. Zhang, J. G, Edirisinghe, M J & Evans, J R G., A catalogue of ceramic injection moulding defects and their causes *Indust Ceram*, **9** (1989) 72–82.
7 Carlsson, R, Shaping of engineering ceramics *Mater Design*, **10** (1989) 10–14.
8. Woodthorpe, J, Edirisinghe, M J & Evans, J. R G, Properties of ceramic injection moulding formulations, III Polymer removal *J Mater Sci*, **24** (1989) 1038–48
9 Wright, J. K, Evans, J R. G & Edirisinghe, M J, Degradation of polyolefin blends used for ceramic injection moulding *J. Amer Ceram Soc*, **72** (1989) 1822–8
10 Szekely, J, Evans, J W. & Sohn, H Y, *Gas-Solid Reactions* Academic Press, NY, 1976, Chapter 4
11 Calvert, P & Cima, M, Theoretical models for binder burnout *J Amer Ceram Soc*, **73** (1989) 575–9
12 Matar, S A., Edirisinghe, M J, Evans, J R G. & Twizell, E. H, The effect of porosity development on the removal of organic vehicle from ceramic or metal mouldings *J. Mater Res*, **8** (1993) 617–25.
13 Cima, M. J, Lewis, J A & Devoe, A D., Binder distribution in ceramic greenware during thermolysis *J Amer Ceram Soc*, **72** (1989) 1192–9
14. Evans, J. R. G, Edirisinghe, M. J, Wright, J K & Crank, J, On the removal of organic vehicle from moulded ceramic bodies, *Proc Royal Soc (London)*, **A432** (1991) 321–40
15 Shaw, H M., Hutton, T J & Edirisinghe, M. J, On the formation of porosity during removal of organic vehicle from injection moulded ceramic bodies *J Mater Sci Lett*, **11** (1992) 1075–7
16 Shaw, H M, Edirisinghe, M J & Holding, S, Binder degradation and redistribution during pyrolysis of ceramic injection mouldings *J Mater Sci Lett.*, **12** (1993) 1227–30
17 Sproson, D W. & Messing, G L. In *Better Ceramics through Chemistry III*, ed C J Brinker, D E Clark & D R. Ulrich. Materials Research Society, PA, 1988, pp 528–37
18 Masia, S, Calvert, P. D, Rhine, W E & Bowen, H K, Effect of oxides during binder burnout during ceramics processing *J Mater Sci.* **24** (1989) 1907–12
19 German, R. M, *Particle Packing Characteristics.* Metal Powder Industries Federation, Princetown, NJ, 1989, pp 275–308
20. Whittlemore, O J, Mercury porosimetry of ceramics *Powder Tech*, **29** (1981) 167
21 Sumita, S., Rhine, W E. & Bowen, H K, Effect of organic dispersants on the dispersion, packing and sintering of alumina *J. Amer. Ceram Soc*, **74** (1991) 2170–4
22 Zheng, J. & Reed, J S, The different roles of forming and sintering on densification of powder compacts *Bull Amer Ceram Soc*, **71** (1992) 1410–16
23 Zheng, J & Reed, J. S, Study of the bimodal pore structure of ceramic powder compacts by mercury porosimetry *J. Am. Ceram Soc*, **75** (1992) 3498–500
24 Cumberland, D J & Crawford, R J, *The Packing of Particles* Elsevier, Amsterdam, 1987, p 60
25 Wright, J K & Evans, J R G, Removal of organic vehicle from moulded ceramic bodies by capillary action *Ceram Int*, **17** (1991) 79–87
26 Zhang, J G, Edirisinghe, M J & Evans, J. R G, The use of modulated pressure in ceramic injection moulding *J. Eur. Ceram. Soc*, **5** (1989) 63–72
27 Zhang, J G, Edirisinghe, M J & Evans, J R G, Initial heating rate for binder removal from ceramic mouldings. *Mater Lett.*, **7** (1988) 15–18
28 Wright, J K, Edirisinghe, M J, Zhang, J G & Evans, J R. G, Particle packing in ceramic injection moulding *J Amer Ceram Soc*, **73** (1990) 2653–8
29 Shaw, H. M & Edirisinghe, M. J, Mobility of powder particles during debinding green ceramic bodies In *Proc 2nd Eur Ceram Soc Conf*, Ausburg, Germany, September 1991, in press
30 Dubinin, M M Physical adsorption of gases and vapours in micropores In *Prog Surf Membr Sci*, Vol. 9, ed D. A Cadenhead, Academic Press, London, 1975, pp 2–3
31 Lowell, S & Shields, J E, *Powder Surface Area and Porosity*. Chapman and Hall, London, 1991, pp 91–3
32 Shaw, T M, Liquid redistribution during liquid phase sintering *J Amer Ceram Soc.*, **69** (1986) 27–34
33 Cima, M J, Dudziak, M & Lewis, J A, Observation of poly(vinyl butyral)-dibutyl phthalate binder capillary migration *J Amer Ceram Soc.*, **72** (1989) 1087–90
34 Zhang, J. G, Edirisinghe, M. J & Evans, J R G, The use of silane coupling agents in ceramic injection moulding. *J Mater Sci*, **23** (1988) 2115–20
35 German, R M, *Powder Injection Moulding* Metal Powder Industries Federation, NJ, 1990, p 301